The Journal of Immunology

Phosphodiesterase 7A-Deficient Mice Have Functional T Cells

Guchen Yang, Kim W. McIntyre, Robert M. Townsend, Henry H. Shen, William J. Pitts, John H. Dodd, Steven G. Nadler, Murray McKinnon and Andrew J. Watson

J Immunol 2003; 171:6414-6420; ;
doi: 10.4049/jimmunol.171.12.6414
http://www.jimmunol.org/content/171/12/6414

The Journal of Immunology is published twice each month by
The American Association of Immunologists, Inc.,
1451 Rockville Pike, Suite 650, Rockville, MD 20852

Print ISSN: 0022-1767 Online ISSN: 1550-6606.

Phosphodiesterase 7A-Deficient Mice Have Functional T Cells

Guchen Yang,[1] Kim W. McIntyre, Robert M. Townsend, Henry H. Shen, William J. Pitts, John H. Dodd, Steven G. Nadler, Murray McKinnon, and Andrew J. Watson

Phosphodiesterases (PDEs) are enzymes which hydrolyze the cyclic nucleotide second messengers, cAMP and cGMP. In leukocytes, PDEs are responsible for depletion of cAMP which broadly suppresses cell functions and cellular responses to many activation stimuli. PDE7A has been proposed to be essential for T lymphocyte activation based on its induction during cell activation and the suppression of proliferation and IL-2 production observed following inhibition of PDE7A expression using a PDE7A antisense oligonucleotide. These observations have led to the suggestion that selective PDE7 inhibitors could be useful in the treatment of T cell-mediated autoimmune diseases. In the present report, we have used targeted gene disruption to examine the role PDE7A plays in T cell activation. In our studies, PDE7A knockout mice (PDE7A$^{-/-}$) showed no deficiencies in T cell proliferation or Th1- and Th2-cytokine production driven by CD3 and CD28 costimulation. Unexpectedly, the Ab response to the T cell-dependent Ag, keyhole limpet hemocyanin, in the PDE7A$^{-/-}$ mice was found to be significantly elevated. The results from our studies strongly support the notion that PDE7A is not essential for T cell activation. ***The Journal of Immunology*****, 2003, 171: 6414–6420.**

Cyclic nucleotide phosphodiesterases (PDEs)[2] catalyze the hydrolysis of second messenger purine nucleotides, 3′, 5′-cAMP and 3′, 5′-cGMP, to their biologically inactive nucleotide 5′-monophosphates (1). Both cAMP and cGMP play a pivotal role in regulating signaling pathways for many essential cellular functions (1–3). In the immune system, cAMP is the primary regulatory cyclic nucleotide (4). It is believed that cAMP broadly suppresses the functions of immune and inflammatory cells (5–6) and a reduction in intracellular cAMP pools is required for cells to effectively respond to extracellular stimuli. This reduction is mediated principally by the action of cell-specific PDEs (4), and PDE inhibitors, such as those selective for PDE4, have been demonstrated to reinforce the cAMP constraint on activation in many immune and inflammatory cells (6–7). This approach to sustaining cAMP levels has proved therapeutically effective, and PDE4 inhibitors, due to their broad anti-inflammatory and bronchodilating effects, are in late-stage clinical development for the treatment of pulmonary diseases, such as asthma and chronic obstructive pulmonary disease (6, 8).

The PDE7 family of high-affinity cAMP-specific PDEs has two members, PDE7A and PDE7B (Refs. 9–13, see Ref. 1 for nomenclature). PDE7A occurs as three alternative splice variants, PDE7A1, PDE7A2, and PDE7A3 (14). PDE7A1 is primarily expressed in lymphoid organs, such as thymus, lymph nodes, spleen, and also peripheral blood T cells and T cell lines (10–12). In contrast, PDE7A2 is highly expressed in skeletal muscle and heart (15) while the PDE7A3 splice variant mRNA is detected in T lymphocytes. Recombinant PDE7A3 proteins have, however, so far failed to show associated PDE enzymatic activity (14). PDE7B is expressed in a number of tissues including brain, heart, and skeletal muscle but significant expression in lymphoid organs is not observed (12–13).

The T cell expression of PDE7A1 has led to the proposal that this PDE may play a broad role in regulating T cell functions. In support of this, Li et al. (16) demonstrated that PDE7A1 protein and enzymatic activity were not detectable in resting peripheral T cells but levels were induced by CD3 × CD28 costimulation. These increases in the PDE7A1 protein and enzymatic activity correlated with a decrease in cAMP levels and an increase in proliferation and IL-2 production. In addition, a PDE7A-specific antisense oligonucleotide, which blocked PDE7A expression, inhibited T cell proliferation and IL-2 production in a protein kinase A-dependent manner. The authors inferred that PDE7A plays an essential role in T cell activation and, therefore, may be an appropriate target for therapeutic intervention in T cell-mediated diseases.

In addition to PDE7A, at least five other PDEs which hydrolyze cAMP–PDE3B, PDE4A, PDE4B, PDE4D, and PDE8A–are reported to be present in peripheral T cells and human T cell lines (14, 17, 18). Although the relative contribution of each of these PDEs to the regulation of T cell function remains unclear, studies using selective PDE inhibitors have established that PDE4 family members, in particular PDE4B and PDE4D, regulate T cell cytokine production and, to a lesser extent, proliferative responses to Ags and mitogens (6).

In the present study, we used mice with a targeted disruption of the PDE7A gene (PDE7A$^{-/-}$) to investigate the role PDE7A plays in T lymphocyte activation. Contrary to the expectation that inactivation of PDE7A would lead to impaired T cell activation, we found that T cell proliferative responses and secreted Th1 cytokine levels (IL-2, IFN-γ, TNF-α) induced by CD3 × CD28 costimulation in the PDE7A$^{-/-}$ mice were comparable to wild-type littermates. A clear phenotypic difference was, however, found in the in vivo Ab response to keyhole limpet hemocyanin (KLH), where the PDE7A$^{-/-}$ mice developed significantly higher mean Ab titers. Our studies do not support the proposal that PDE7A plays a critical role in regulating T cell proliferation.

Immunology and Inflammation Drug Discovery, Bristol-Myers Squibb Pharmaceutical Research Institute, Princeton, NJ 08543

Received for publication August 13, 2003. Accepted for publication October 9, 2003.

The costs of publication of this article were defrayed in part by the payment of page charges. This article must therefore be hereby marked *advertisement* in accordance with 18 U.S.C. Section 1734 solely to indicate this fact.

[1] Address correspondence and reprint requests to Dr. Guchen Yang, Bristol-Myers Squibb Pharmaceutical Research Institute, P.O. Box 4000, Princeton, NJ 08543-4000. E-mail address: guchen.yang@bms.com

[2] Abbreviations used in this paper: PDE, phosphodiesterase; CBA, cytometric bead array assay; KLH, keyhole limpet hemocyanin.

0022-1767/03/$02.00

Materials and Methods

Mice

The PDE7A knockout mice were generated by Lexicon Genetics (Woodlands, TX) using random retroviral gene trapping in embryonic stem cells as previously described (19). The PDE7A$^{-/-}$ mice were born at Mendelian ratios and were fertile. The mice were examined for diverse phenotypic parameters including gross and microscopic pathology and no discernible phenotype was found. However, ~50% of PDE7A$^{-/-}$ mice exhibited a lower percent body fat (~10%) than the PDE7A$^{+/-}$ and PDE7A$^{+/+}$ mice which may be the consequence of a nonfunctional PDE7A2. Three pairs of PDE7A heterozygous (+/−) mice with C57BL/6 × 129/Ola genetic background were supplied and interbred to generate PDE7A-deficient mice and wild-type littermates. All −/−, +/−, and +/+ mice used for experiments were progeny of the −/−, +/−, and +/+ mice, respectively, and were maintained in a specific pathogen-free mouse facility. Both male and female mice were used for studies at 6–20 wk of age. All studies involving animals were reviewed and approved by the Institutional Animal Care and Use Committee.

Genotyping PDE7A$^{-/-}$ mice

The PDE7A$^{-/-}$ mice used as breeding stocks were identified by PCR. Mouse tail DNA was extracted using proteinase K (Qiagen, Valencia, CA). Briefly, a 0.5–1 cm piece of tail was digested at 60°C for overnight in tail lysis buffer (pH 8.0) containing Tris (50 mM), EDTA (50 mM), NaCl (100 mM), DTT (5 mM), spermidine (50 μM), and 1% sarkosyl (v/v). The genomic DNA was precipitated, washed, and then dissolved in Tris-EDTA buffer (10 mM Tris and 1 mM EDTA, pH 8.0) for further use. Three primers, named a, b, and LTR2, were designed based on the genomic sequence surrounding the insertion site and the sequence of vector-specific oligonucleotide (see Fig. 1*A*). They were: primer a, 5′-TCACTCCACAAATG CACTCAC-3′; primer b, 5′-CCTGCTTTCCAATGGCAAGTG-3′; and primer LTR2, 5′-AAATGGCGTTACTTAAGCTAGCTTGC-3′. A pool of three primers was used in PCRs for screening tail DNA. PCR was performed with the following cycle parameters: 94°C/4 min, 1 cycle; 94°C/30 s, 55°C/30 s, 72°C/30 s, 30 cycles; and 72°C/5 min, 1 cycle. PCR products were separated in a 1.2% agarose gel. The wild-type allele gave PCR products of 320 bp using primers a + b. The mutant PDE7A allele gave PCR products of 190 bp using primers LTR2 + b (see Fig. 1*B*).

RT-PCR for PDE7A mRNA expression

Total RNA was extracted from spleen and skeletal muscle using an RNeasy kit (Qiagen) according to the manufacturer's instructions. Reverse transcription was performed as follows: 1.5 μg of RNA with 4 μl of random primer (1 μg/μl) were incubated at 65°C for 2 min. After incubation, the mixture was immediately cooled on ice, and then 20 U reverse transcriptase (Invitrogen, Carlsbad, CA), 10 U RNase inhibitor, 500 μM dNTP, 500 μM DTT, and 4 μl 5× transcriptase dilution buffer were added. The final volume was 20 μl. The cDNA synthesis reactions were conducted at 42°C for 1 h, followed by heat inactivation. Primers used to amplify cDNA of full-length PDE7A were: 5′-GCAGAGACGTGGAGCTATTTC-3′ (sense) and 5′-CTCAAATGCAGCATTGGCATC-3′ (antisense). Primers for the catalytic domain were: 5′-AGACGTTACTCAGGCCATG CACTGTTACTT-3′ (sense) and 5′-AGAACCAAATGCCTATGTCT GCCATCGTCA-3′ (antisense) and primers for 5′ truncated PDE7A were: 5′-ATGGAAGTATGCTACCAGCTG-3′ (sense) and 5′-TGGG TGATCCAGATCGTGAGT-3′ (antisense). PCR was performed as described above.

Quantitative PCR for PDE7A mRNA expression

PDE7A expression patterns were determined by quantitative PCR. PCR primers were designed by the Primer3 program (Whitehead Institute for Biomedical Research, Cambridge, MA). SYBR green PCR core reagents were purchased from Applied Biosystems (Foster City, CA). Real-time PCR was performed on a ABI Prism 5700 Sequence Detection System (Applied Biosystems). PCR samples were incubated at 95°C for 15 s, 55°C for 20 s, and 75°C for 1 min for 40 cycles. Real-time PCR primers spanning the insertion region (OmniBank sequence tag primers) were 5′-GT GTTAATCAGCCGTTTCTTATT-3′ (sense) and 5′-CAAAGCACCTAT CTGAGCCT-3′ (antisense). Real-time PCR primers for catalytic domain region (catalytic domain primers) were 5′-AGTCTATTGCCAACATC CAGATTG-3′ (sense) and 5′-GAAAACCTGGCCCACTCTGTAA-3′(antisense). Following PCR and data collection, dissociation curve studies were performed to confirm the homogeneity of the PCR product. In addition, PCR samples were analyzed by agarose gel electrophoresis to confirm the size of the PCR product. All data were normalized using murine housekeeping gene HPRT to ensure equal initial sample RNA input. The normalized data were presented as fold changes over the data from wild-type mouse sample.

Cell lysate preparation for PDE assay

Cells from lymph nodes of PDE7$^{-/-}$, PDE7$^{+/+}$, and C57BL/6 control mice were obtained by dissociating lymph nodes through nylon screens. The resuspended cells were washed once and suspended in complete medium RPMI 1640 (RPMI 1640 supplemented with 10% FCS, penicillin/streptomycin, 2 mM glutamine, and 50 μM 2-ME). The cells were activated using Abs to CD3 (145-2C11, 1 μg/ml) and CD28 (3N7, 2 μg/ml) in T25 tissue culture flasks using standard culture conditions. After 72 h, the cells were washed, pelleted, and lysed at 4°C for 30 min in a hypotonic buffer containing Tris (40 mM) and EDTA (50 μM), pH 7.4, supplemented with pepstatin (1 μM), leupeptin (5 μg/ml), prefabloc (200 μM), and 0.5% Triton X-100 (v/v). The supernatants were collected following microcentrifugation at 13,000 rpm, diluted with an equal volume of glycerol and stored at −20°C for further use.

Assay of PDE activities

PDE activities were measured using the PDE Scintillation Proximity Assay (SPA) according to the manufacturer's protocol (Amersham Pharmacia Biotech, Piscataway, NJ). Briefly, aliquots of the cell lysates were diluted in SPA buffer, (50 mM Tris, pH 7.5, 8.3 mM $MgCl_2$, 1.7 mM EDTA, 0.5 mg/ml BSA) in the absence or the presence of selective PDE inhibitors in a white flat-bottom 96-well plate. The reactions were initiated by the addition of 0.1 μCi [^{3}H]cAMP per well to give a total volume of 100 μl. Following a 60-min incubation at room temperature, the reactions were stopped by adding 50 μl of SPA beads supplemented with an excess (5–10 mM) cold cAMP. The plate was gently shaken for 5 min, the beads allowed to settle for 20 min, and then counted on TopCount (Packard Instrument, Meriden, CT). Average counts of triplicate results from each assay were determined and the corresponding background levels for cAMP were subtracted. PDE activity was expressed as fmol cAMP hydrolyzed per million cells in 60 min. In this assay format, PDE7 activity was assessed using a highly selective PDE7 inhibitor, BMS-586353 (PDE7 IC_{50} 8 nM). The selectivity of BMS-586353 is 3722-fold against PDE1, 6277-fold against PDE3, >1250-fold against PDE4, 1231-fold against PDE5, and 553-fold against PDE6, based on the fold differences of the IC_{50} values. PDE3 activity was measured using the selective PDE3 inhibitor, cilostamide (PDE3 IC_{50} 5 nM; BioMol, Plymouth Meeting, PA), and PDE4 activity was measured using the selective PDE4 inhibitor, cilomilast (PDE4 IC_{50} 45 nM) (20). All inhibitors were used at a final concentration equal to their IC_{50} values and, hence, the contribution of each PDE was calculated as: (PDE activity in the absence of the specific inhibitor − PDE activity in the presence of the specific inhibitor) × 2.

Flow cytometry

Cells from lymph nodes and spleens were obtained by dissociating lymph nodes or spleens through nylon screens. The RBC in spleen preparations were removed by Red Blood Cell Lysis Solution (Sigma-Aldrich, St. Louis, MO). Single-cell suspensions from lymph nodes and spleens were prepared in a 96-well plate (2×10^5 cells/well) in complete medium RPMI 1640. Before staining with specific Abs (all Abs were purchased from BD Biosciences, San Diego, CA), the cells were incubated at 4°C for 15 min with purified anti-CD16 mAb to block FcRs. The following Abs were used to detect leukocyte subsets: 145−2C11 for CD3, GK1.5 for CD4, 53−6.7 for CD8, PK136 for NK1.1, RA3−6B2 for B220 and M1/70 for CD11b. The PE-conjugated mAbs were added to each well in FACS buffer (PBS containing 0.1% BSA and 0.2% NaN_3) and incubated at 4°C for 30 min. Following two washes with FACS buffer, cells were resuspended in FACS buffer containing 1% paraformaldehyde. Samples were analyzed by using CellQuest software on a BD Biosciences FACSort (BD Biosciences).

In vitro T cell proliferation

Lymph node cells and splenocytes were activated by anti-CD3 mAb (145-2C11, 1 μg/ml) with or without anti-CD28 mAb (3N7, 2 μg/ml) in complete medium RPMI 1640 in 96-well flat-bottom plates (2×10^5 cells/well). Following a 72-h incubation at 37°C in 5% CO_2 and 90% humidified air, the cultures were pulsed for 8 h with [^{3}H]thymidine (1 μCi; NEN, Boston, MA). The cells were then harvested on a Packard cell harvester using Packard GF/C plates. After addition of scintillation mixture into the GF/C plates, incorporated radioactivity was determined using a TopCount. The effect of the PDE4 inhibitor, cilomilast, on T cell proliferation was tested using a similar protocol. Lymph node cells and splenocytes were activated by combined anti-CD3 mAb (145-2C11, 1 μg/ml) and anti-CD28

mAb (3N7, 2 μg/ml). The inhibitor was added into the wells in complete medium RPMI 1640. The assay was incubated for 72 h at 37°C and proliferation measured using [^{3}H]thymidine incorporation. Percentage of inhibition = (1 − cpm in the presence of cilomilast/cpm in the absence of cilomilast) × 100. When purified T cells were used in assays, mixed cells from lymph nodes and spleens were incubated on plastic (T75 tissue culture flask, 1×10^7 cells/ml) for 60 min to remove the adherent monocytes and macrophages. After incubation, the nonadherent cells were twice depleted of surface Ig$^+$ cells using Dynabeads M450 (Dynal, Lake Success, NY) for 60 min on a rotator at 4°C. The ratio of beads to target cells was 4:1. Following two cycles of magnetic depletion, the remaining cells were washed once in complete medium RPMI 1640. The resulting purified T cells were stimulated on an anti-CD3 (1 μg/ml) coated 96-well plate (2×10^5 cells/well) with or without soluble anti-CD28 at 2 μg/ml final for 72 h.

Quantitation of T cell cytokines

Cell cultures were set up as described above except in T25 tissue culture flasks. Supernatants were harvested at the indicated times. Standard ELISA kits (BD Biosciences) and the FACS-based multiplex cytometric bead array assays (CBA; BD Biosciences) were used to measure IL-2, IL-4, IL-5, IFN-γ and TNF-α. For ELISA, cytokine levels were determined by interpolation of standard curves using SOFTmaxPRO Quantitation software (Molecular Devices, Sunnyvale, CA). For the CBA, cytokine levels were calculated using the manufacturer supplied CBA analysis software package, FACSComp (BD Biosciences).

KLH-induced Ab response in vivo

PDE7A$^{-/-}$ and PDE7A$^{+/+}$ mice were immunized i.p. with a single injection of 250 μg of KLH (Pierce, Rockford, IL) in PBS. Blood was drawn on days 7, 14, and 21 and analyzed for serum anti-KLH IgG by ELISA. Briefly, 96-well plates were coated with KLH in PBS, blocked, and serial dilutions of test serum samples were added. Captured anti-KLH Abs were detected using HRP-conjugated Ab specific for mouse IgG (Southern Biotechnology Associates, Birmingham, AL), and TMB microwell peroxidase substrate system (Kirkegaard & Perry Laboratories, Gaithersburg, MD). ODs were quantitated in a SpectraMax Plus ELISA plate reader (Molecular Devices). A pooled serum from KLH-immunized C57BL/6 mice was used as an internal positive control in each ELISA and the data are expressed as a ratio of the titer of the test serum to the titer of the pooled C57BL/6 serum.

Statistical analysis

Mean and SE values from each triplicate set as well as *t* test comparisons were derived by using GraphPad Prism software from GraphPad Software (San Diego, CA). A p value <0.05 was considered statistically significant.

Results

PDE7A transcripts and enzymatic activity

PDE7A$^{-/-}$ mice were generated using random retroviral gene trapping in embryonic stem cells (19). Genomic sequencing established that the retroviral vector (7.4 kb), inserted into the intron of mouse PDE7A corresponding to the intron of human PDE7A between exons 5 and 6. The resulting integration caused disruption of full-length transcripts of the PDE7A gene and the production of two fusion transcripts, a 5′ portion with *βgeo* and a 3′ portion with *puro* (Fig. 1, *A* and *C*). Consistent with this, neither full-length PDE7 mRNA transcripts nor PDE7 transcripts spanning the insertion site could be detected in spleen cells (Fig. 1*D* and Table I) or CD3 × CD28-activated lymph node cells (data not shown) using standard RT-PCR and real-time quantitative RT-PCR procedures. As expected, PDE7 transcripts 5′ to the insert could be detected while PDE7 transcripts 3′ to the insert were reduced by >95% (Table I).

Based on a published site-directed mutagenesis study (21) and the crystal structure of the highly homologous catalytic domain of PDE4B (22), it would be predicted that the retroviral insertion disrupts the catalytic domain of PDE7A and separates the exons encoding the metal binding residues essential for catalytic function from the substrate binding pocket. Therefore, neither 5′ nor 3′ fusion transcript could direct synthesis of a functional catalytic domain. To confirm this prediction, we conducted experiments to

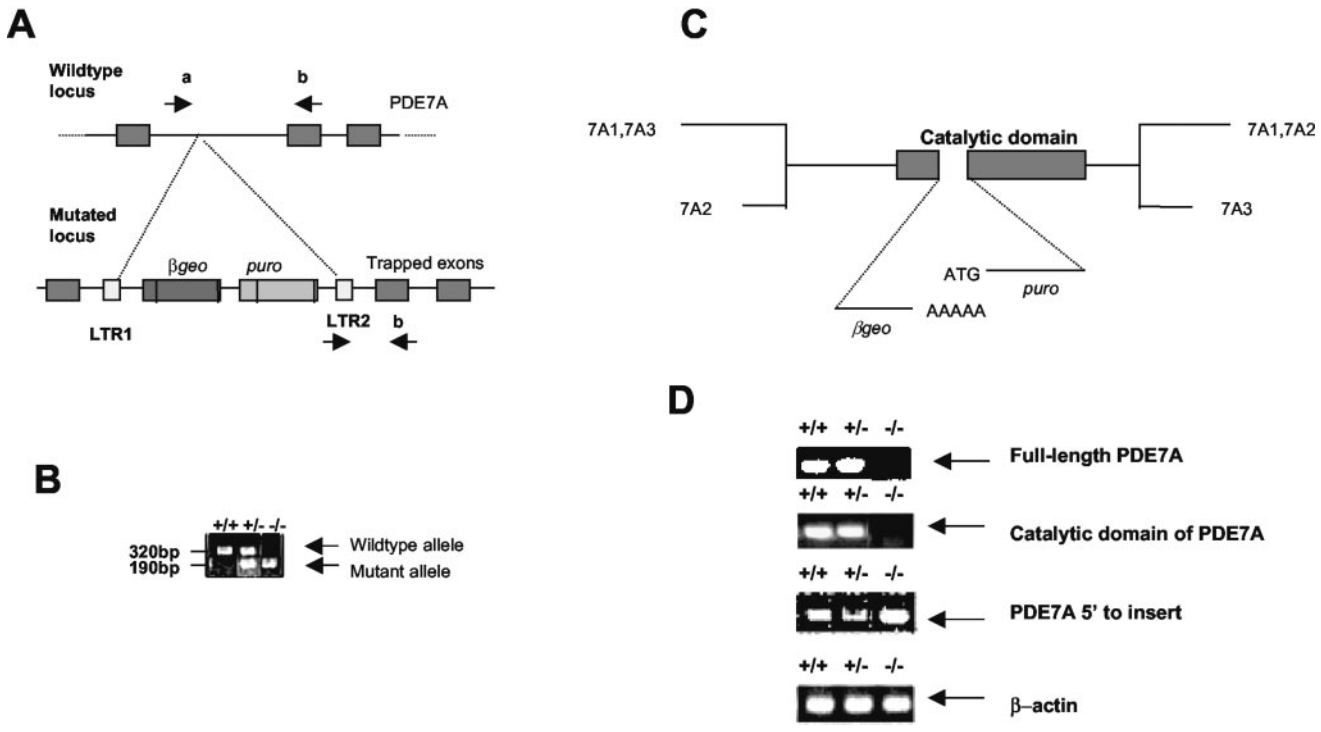

FIGURE 1. Characterization of PDE7A knockout mice. *A*, Schematic representation of retroviral integration and primer design for PCR genotyping. *B*, PCR products from genomic DNA. A pool of three PCR primers (a, b, and LTR2) was used to screen tail DNA (wild-type (+/+), heterozygous (+/−), and homozygous knockout (−/−)). *C*, Schematic representation of PDE7 transcripts. *D*, RT-PCR for PDE7A mRNA expression. Total RNA from spleen was used. For primer sequences, see *Materials and Methods*.

Table I. *Relative levels of mRNA transcripts*[a]

	Primers Targeted 5′ and 3′ to the Insert Site	Primers Targeted 3′ of the Insert
	OST	CA
PDE7A$^{+/+}$	1.0000	1.0000
PDE7A$^{+/-}$	0.2269	0.2859
PDE7A$^{-/-}$	0.0019	0.0440

[a] Data shown represent the mean of three individual mice. OST, OmniBank sequence tag; CA, catalytic domain.

examine PDE7 enzymatic activity in PDE7A$^{-/-}$ mice by using a highly selective PDE7 inhibitor, BMS-586353. Consistent with expectations, in three separate experiments and using a total of 15 PDE7A$^{-/-}$ mice, PDE7A activity in lysates from CD3 × CD28-activated lymph node cells was found to be at background levels whereas PDE7A activity was readily detected in wild-type mice and usually constituted 12–24% of the total cAMP PDE activity (data not shown).

We also attempted to determine whether a compensatory change in relative levels of PDE3 and PDE4 activity had occurred in the PDE7A$^{-/-}$ mice. Fig. 2 shows the results of an experiment where the contribution of PDE3 and PDE4 to the total PDE activity in the activated lymph node cell lysate was determined using highly selective PDE inhibitors. On a per cell basis, PDE7A$^{-/-}$ mice showed a lower total level of cAMP PDE activity but the levels of PDE3, PDE4 and the residual non-PDE3, PDE4, PDE7 activity (PDEX) were comparable between the six mice in each group.

Immunological phenotyping

The subpopulations of cells resident in lymph node and spleen of the PDE7A$^{-/-}$ mice appeared essentially normal. A FACS analysis of lymph node cells and splenocytes from PDE7A$^{-/-}$ and PDE7A$^{+/+}$ mice revealed no significant difference in the number of total and CD4$^+$ T lymphocytes and no difference in the number of NK cells (NK1.1$^+$), B lymphocytes (B220$^+$), and macrophages (CD11b$^+$). However, PDE7A$^{-/-}$ mice contained significantly fewer CD8$^+$ T cells than their wild-type littermates in lymph nodes ($p < 0.05$) but not in spleens (Table II) and peripheral blood (data not shown).

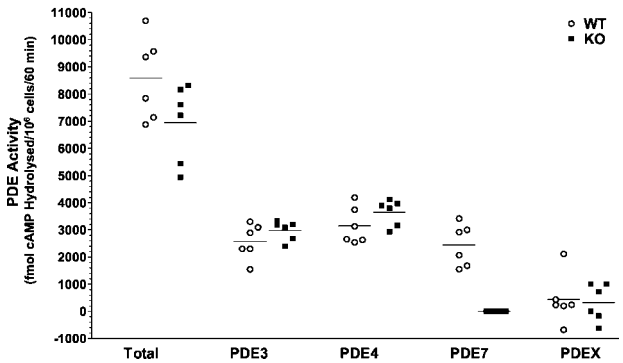

FIGURE 2. cAMP PDE activity in lymph node cell lysates. Lymph node cells from PDE7A$^{+/+}$ and PDE7A$^{-/-}$ mice were activated by CD3 × CD28 stimulation for 72 h. PDE3, PDE4, and PDE7 activities in cell lysates were quantitated using highly selective inhibitors, as described in *Materials and Methods*. Data shown are from six PDE7A$^{+/+}$ (wild type (WT), ○) and PDE7A$^{-/-}$ (knockout (KO), ■) mice. PDE activity expressed as fmol cAMP hydrolyzed per million cells in 60 min.

T cell activation in PDE7A$^{-/-}$ mice

It is well-established that signaling by both TCR and CD28 costimulatory molecules is sufficient for optimal activation of T lymphocytes in vivo and in vitro (23). Therefore, we investigated the CD3- and CD3 × CD28-dependent T cell proliferation and cytokine production in PDE7A$^{-/-}$ mice. In a series of experiments, T cells purified from lymph nodes and spleens were stimulated with varying amounts of immobilized anti-CD3 mAb alone or in combination with an anti-CD28 mAb. Proliferation by day 3 was measured using [^{3}H]thymidine incorporation. As shown in Fig. 3*A*, T cells from PDE7A$^{-/-}$ mice proliferated as well as those from PDE7A$^{+/+}$ wild-type control regardless of the nature of the stimulus. The combined results of additional experiments where lymph node cells (seven experiments) and spleen cells (five experiments) were costimulated with anti-CD3 × anti-CD28 are shown in Fig. 3*B*. In contrast to that of lymph node cells, the proliferation of spleen cells from PDE7A$^{-/-}$ mice was slightly decreased as compared with that from PDE7A$^{+/+}$ mice but this decrease was not statistically significant ($p = 0.3$). Overall, our data indicate that, regardless of the tissue source of T cells or the stimulus used, no significant reduction in the proliferative response of the T cells from the PDE7A$^{-/-}$ mice was observed. Because PDE4 inhibitors have been previously shown to suppress T cell proliferation (24, 25), as a control, we tested a PDE4 inhibitor, cilomilast, in T cell proliferation assays in cells derived from wild-type and knockout mice. In agreement with published results, cilomilast, in a dose-dependent manner, inhibited CD3 × CD28-driven proliferation of lymph node cells and splenocytes from either PDE7A$^{+/+}$ or PDE7A$^{-/-}$ mice (Fig. 3*C*). The differences in the level of inhibition between groups of PDE7A$^{+/+}$ mice and PDE7A$^{-/-}$ mice were not statistically significant (all points, $p = 0.06–0.8$). These data suggest that our experimental conditions could detect subtle effects on proliferation through PDE inhibition.

Although inactivation of the PDE7A gene does not appear to exert a significant effect on T cell proliferative responses, activated T cells also produce multiple cytokines which are critical mediators of T cell function. To determine whether PDE7A plays a role in the regulation of cytokines, we compared the production of Th1 and Th2 cytokines by activated T cells from PDE7A$^{-/-}$ and PDE7A$^{+/+}$ mice. Supernatants were collected from spleen cells, lymph node cells, and purified T cells activated with anti-CD3 and anti-CD28 Abs and cytokines were measured using ELISA and CBAs. In these experiments, no differences in the production of the Th1 cytokines, IL-2, IFN-γ, or TNF-α between PDE7A$^{-/-}$ and PDE7A$^{+/+}$ mice could be detected (Fig. 4, $p = 0.9$, $p = 0.5$, and $p = 0.5$, respectively). Levels of the Th2 cytokines, IL-4, IL-5 and IL-13, were very low in most culture supernatants, making accurate comparisons difficult. However, as with the Th1 cytokines, no significant differences were seen between PDE7A$^{-/-}$ and PDE7A$^{+/+}$ mice (data not shown).

In vivo Ab responses

The role PDE7A plays in the development of T-dependent Ab responses was investigated using KLH immunization. Mice were given a single i.p. injection of KLH and the developing Ab titers monitored by Ag-specific ELISA. The combined results of two similar experiments are shown in Fig. 5. The scatter plot shows that the PDE7A$^{-/-}$ mice had developed clearly higher titers by days 7, 14, and 21 postimmunization than PDE7A$^{+/+}$ mice ($p <$ 0.001 at all three time points).

Table II. *Cell populations in PDE7A$^{+/+}$ and PDE7A$^{-/-}$ mice*[a]

	CD3$^+$	CD4$^+$	CD8$^+$	NK1.1$^+$	B220$^+$	CD11b$^+$
Lymph node						
PDE7A$^{+/+}$	60.4 ± 2.8	44.2 ± 1.3	31.9 ± 0.4	2.4 ± 0.1	43.4 ± 3.7	10.1 ± 0.4
PDE7A$^{-/-}$	52.7 ± 0.8	40.6 ± 1.9	25.9 ± 1.5[b]	3.2 ± 0.6	48.4 ± 0.5	12.2 ± 0.7
Spleen						
PDE7A$^{+/+}$	28.7 ± 2.7	26.6 ± 1.8	16.7 ± 2.2	6.7 ± 1.4	67.8 ± 2.3	20.4 ± 0.8
PDE7A$^{-/-}$	24.2 ± 2.8	25.0 ± 1.9	14.8 ± 2.1	5.8 ± 0.7	69.1 ± 0.5	21.0 ± 2.2

[a] Data shown represent the mean ± SD of percentages of three individual mice.
[b] $p < 0.05$.

Discussion

Using mice with a targeted disruption in the PDE7A gene, we report here for the first time that PDE7A is not essential for activation of T lymphocytes. The T cells from PDE7A$^{-/-}$ mice were functional in proliferative responses and cytokine production in vitro and functional in a T cell-dependent Ab response in vivo.

Although PDE7A was discovered ~10 years ago (9) and the splice variant, PDE7A1, was found expressed in several human T cell lines 3 years later (10), the role of PDE7A in T cell function remains largely unknown. Li et al. (16) reported that expression of PDE7A is up-regulated in human T cells upon costimulation with CD3 and CD28. They further proposed a central role for PDE7A in T cell activation as a result of experiments using an antisense oligonucleotide specific for PDE7A to inhibit CD3 × CD28-driven T cell proliferation and IL-2 production in vitro. However, another report indicated that the identical antisense oligonucleotide was unable to induce a statistically significant reduction of IL-13 in CD3 × CD28-activated human T cells (26). Using PDE7A$^{-/-}$ mice, our data demonstrated that inactivation of PDE7A causes no significant changes in T cell proliferation or IL-2 production. The lack of phenotypic differences in PDE7A$^{-/-}$ mice was observed regardless of how T cells were stimulated, by combined anti-CD3 and anti-CD28 or by anti-CD3 alone, and regardless of the concentrations of anti-CD3 used. In addition, no clear preferential impact on either Th1 or Th2 cytokines was found. Furthermore, T cells derived from either PDE7A$^{+/+}$ or PDE7A$^{-/-}$ mice were

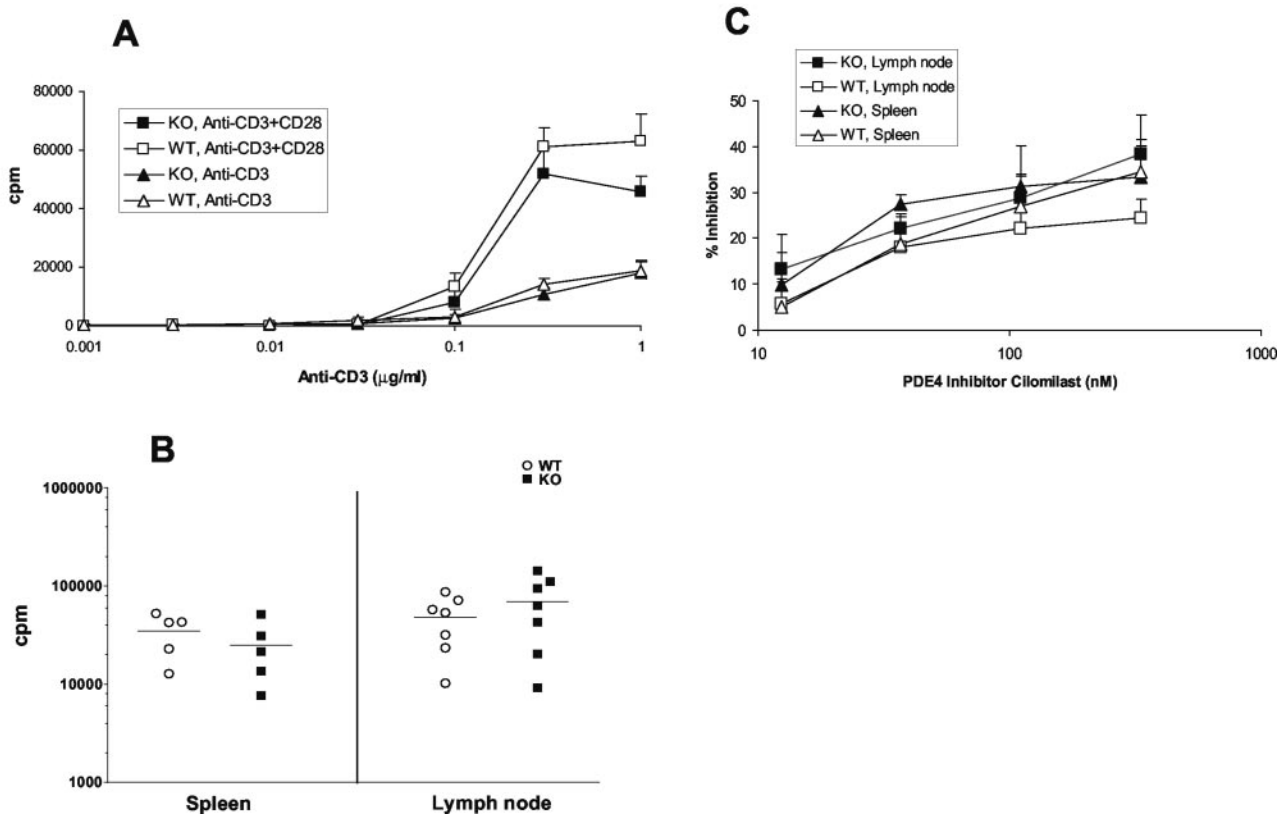

FIGURE 3. Comparison of T cell proliferation between PDE7A$^{+/+}$ and PDE7A$^{-/-}$ mice. *A*, [^{3}H]Thymidine incorporation by T lymphocytes purified by negative selection from PDE7A$^{-/-}$ mice (KO, closed symbols) and PDE7A$^{+/+}$ mice (WT, open symbols) and stimulated for 72 h by titrated levels of anti-CD3 mAb in the presence or absence of anti-CD28 mAb (2 μg/ml). *B*, Combined results from independent experiments where spleen ($n = 5$) and lymph node cells ($n = 7$) were stimulated by anti-CD3 (1 μg/ml) and anti-CD28 (2 μg/ml) for 72 h. Each symbol represents the proliferation level from a culture of cells pooled from two mice. *C*, Effect of PDE4 inhibitor, cilomilast, on T cell proliferation. Lymph node cells and splenocytes from PDE7A$^{-/-}$ mice (KO, closed symbols) and PDE7A$^{+/+}$ mice (WT, open symbols) were activated by combined anti-CD3 mAb (1 μg/ml) and anti-CD28 mAb (2 μg/ml) in the presence or absence of cilomilast for 72 h. Each symbol represents the proliferation level from a culture of cells pooled from two mice. The proliferation was measured using [^{3}H]thymidine incorporation. Percentage of inhibition = (1 − cpm in the presence of cilomilast/cpm in the absence of cilomilast) × 100.

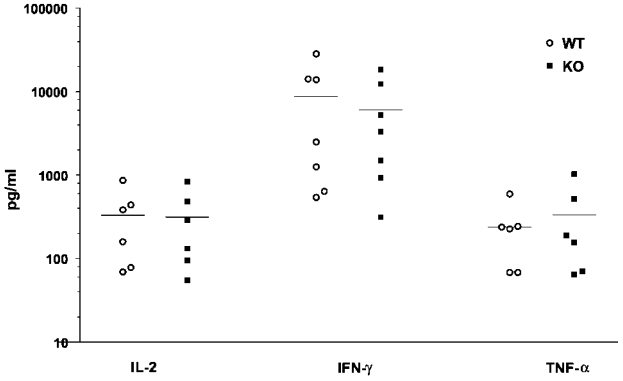

FIGURE 4. Comparison of cytokine production between PDE7A$^{+/+}$ and PDE7A$^{-/-}$ mice. Lymph node cells from PDE7A$^{-/-}$ mice (KO, ■) and PDE7A$^{+/+}$ mice (WT, ○) were activated by anti-CD3 (1 μg/ml) and anti-CD28 (2 μg/ml) for 24 h and cytokine levels in supernatants were measured by ELISA or CBAs. Each symbol represents the cytokine level from a culture of cells pooled from two mice.

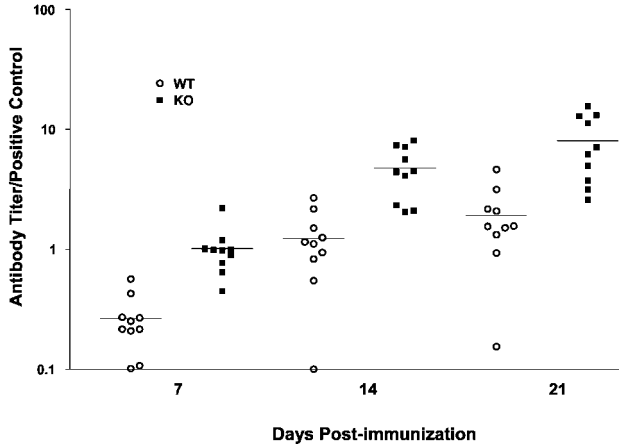

FIGURE 5. Anti-KLH Ab response in PDE7A$^{-/-}$ mice. PDE7A$^{-/-}$ mice (KO, ■, $n = 10$) and PDE7A$^{+/+}$ mice (WT, ○, $n = 10$) were injected i.p. with a single dose of KLH. The Ab titers were monitored at days 7, 14, and 21 post immunization by ELISA specific for anti-KLH IgG. Values of p between KO and WT at days 7, 14, and 21 were 0.0001, 0.0002, and 0.0009, respectively. The results are combination of two independent experiments.

equally sensitive to the effects of the PDE4 inhibitor cilomilast in proliferation assays. Although this inhibitor provides an important positive control in these proliferation assays, the data also suggest no enhanced sensitivity of PDE7-deficient T cells to the effects of PDE4 inhibition.

It is not clear why our data are in disagreement with those of Li et al. (16) who demonstrated the apparent importance of PDE7 in regulating human T cell proliferation through the use of antisense techniques. It is formally possible that there are species differences in the role PDE7 plays in human vs mouse T cell function, or that redundant mechanisms compensate for the congenital deficiency of PDE7A in mice. Alternatively, recent publications suggest that the use of naked oligonucleotides to deliver sequence-specific effects in cells, as used by Li et al., should be avoided due to their poor ability to target a specific cellular mRNA and their sequence-nonspecific toxicities (27). It is possible that these nonspecific effects could account for the inhibitory activities observed using antisense approaches.

Consistent with our observations, several lines of evidence suggest that other PDEs, in particular members of the PDE4 family, may exert dominant control over the cAMP pools that regulate TCR-mediated activation (17). It has been shown that, besides PDE7A, at least five other PDEs catalyze the hydrolysis of cAMP in human T cells (14, 17–18). The PDE4 family members, PDE4A, PDE4B, and PDE4D are reported to be the major isozymes that contribute ~65% of the total PDE activity (17). In agreement with previous estimations, we found that PDE7A accounted for ~10–25% of total PDE activity, even in CD3 × CD28-activated T cells. The enzymatic activity of PDE4 in human T cells can be translated into functional activity. Selective PDE4 inhibitors reduce proliferation of peripheral T lymphocytes induced by PHA (17, 28), specific Ag (29), a combination of phorbol ester and anti-CD3 Ab (28), or anti-CD3 and anti-CD28 Abs (25) up to 60–80%. Although selective PDE3 inhibitors have little effect on their own, they enhance the actions of PDE4 inhibitors (17). One study showed that in the presence of PDE3 and PDE4 inhibitors, an almost complete inhibition of T cell proliferation was obtained (25). In a similar fashion, IL-2 and IFN-γ production of human T cells was inhibited by either PDE4 inhibitors or combination of PDE4 and PDE3 inhibitors (17, 25). Although several selective PDE7 inhibitors have been identified, their effects on T cell function have not been reported (30, 31). In our hands, selective PDE7 inhibitors do not inhibit CD3 × CD28-driven proliferation or IL-2 production of human or mouse T lymphocytes (data not shown). These results imply that in T cells PDE7A plays only a minor role in regulating the cAMP pools which influence proliferation and cytokine production.

PDE7A may regulate a cAMP pool that is not crucial for TCR-mediated activation but may alter other T cell functions. Many PDEs have been shown to target subcellular components and associate with specific signaling proteins (32, 33). As a result, each PDE may have localized control of a cAMP pool or compartmentalization of cell functions. For instance, PDE4D was shown to be recruited to the G protein-coupled β2-adrenergic receptors through signal scaffolding protein β-arrestins (34). The association of PDE4D to β2-adrenergic receptors resulted in desensitization of the receptors. One can speculate that PDE7A may play an important role in the development of memory T cells (35) or the regulation of activation-induced apoptosis in T lymphocytes (36) since it has been shown that cAMP is involved in these aspects of T cell function.

PDE7A$^{-/-}$ mice exhibited an elevated Ab response, suggesting that PDE7A may play a nonredundant role in cAMP signaling events other than those associated with T cell activation. It is not clear whether the T cells in PDE7A$^{-/-}$ mice have accentuated Th2 function or that B cells themselves are hyperactive to secrete Abs. However, we did not see an obvious shift from Th1 to Th2 cytokines (IL-2, IFN-γ, and TNF-α vs IL-4, IL-5, and IL-13) in vitro. Although PDE7A protein has been shown to be expressed in normal human B cells and B cell leukemia lines (37), its role in Ab production remains to be determined. It is possible that inactivation of PDE7A may promote B lymphocyte class switching to IgG rather than Ab production. Clearly, more experiments are needed to explain the phenotype of elevated Ab production.

In summary, the T cells from PDE7A$^{-/-}$ mice were found to be functional and without obvious phenotypic deficiencies in terms of in vitro T cell proliferation and cytokine production. Unexpectedly, T cell-dependent Ab production against KLH was elevated in PDE7A$^{-/-}$ mice. Our data show that inactivation of PDE7A does not suppress T cell-mediated immune responses but appears to enhance humoral immune responses.

Acknowledgments

We gratefully thank Karen L. Donaldson, Deborah Lee, Pin Lu, and Jennifer Postelnek for their technical assistance and Gary Starling for his contributions to the PDE7 program.

References

1. Beavo, J. A. 1995. Cyclic nucleotide phosphodiesterases: functional implications of multiple isoforms. *Physiol. Rev. 75:725*.
2. Mehats, C., C. B. Andersen, M. Filopanti, S. L. Jin, and M. Conti. 2002. Cyclic nucleotide phosphodiesterases and their role in endocrine cell signaling. *Trends Endocrinol. Metab. 13:29*.
3. Houslay, M. D. 1998. Adaptation in cyclic AMP signalling processes: a central role for cyclic AMP phosphodiesterases. *Semin. Cell Dev. Biol. 9:161*.
4. Essayan, D. M. 1999. Cyclic nucleotide phosphodiestase (PDE) inhibitors and immunomodulation. *Biochem. Pharmacol. 57:965*.
5. Kammer, G. M. 1988. The adenylate cyclase-cAMP-protein kinase A pathway and regulation of the immune response. *Immunol. Today 9:222*.
6. Torphy, T. J. 1998. Phosphodiesterase isozymes: molecular targets for novel antiasthma agents. *Am. J. Respir. Crit. Care Med. 157:351*.
7. Peachell, P. T., B. J. Undem, R. P. Scheimer, D. W. MacGlashan, Jr., L. M. Lichtenstein, L. B. Cieslinski, and T. J. Torphy. 1992. Preliminary identification and role of phosphodiesterase isozymes in human basophils. *J. Immunol. 148:2503*.
8. Compton, C. H., J. Gubb, R. Nieman, J. Edelson, O. Amit, A. Bakst, J. G. Ayres, J. P. Creemers, G. Schultze-Werninghaus, C. Brambilla, N. C. Barnes, for the International Study Group. 2001. Cilomilast, a selective phosphodiesterase 4 inhibitor for treatment of patients with chronic obstructive pulmonary disease: a randomised, dose-ranging study. *Lancet 358:265*.
9. Michaeli, T., T. J. Bloom, T. Martins, K. Loughney, K. Ferguson, M. Riggs, L. Rodgers, J. A. Beavo, and M. Wigler. 1993. Isolation and characterization of a previously undetected human cAMP phosphodiesterase by complementation of cAMP phosphodiesterase-deficient *Saccharomyces cerevisiae*. *J. Biol. Chem. 268:12925*.
10. Bloom, T. J., and J. A. Beavo. 1996. Identification and tissue-specific expression of PDE7 phosphodiesterase splice variants. *Proc. Natl. Acad. Sci. USA 93:14188*.
11. Wang, P., P. Wu, R. W. Egan, and M. M. Billah. 2000. Cloning, characterization, and tissue distribution of mouse phosphodiesterase 7A1. *Biochem. Biophys. Res. Comm. 276:1271*.
12. Hetman, J. M., S. H. Soderling, N. A. Glavas, and J. A. Beavo. 2000. Cloning and characterization of PDE7B, a cAMP-specific phosphodiesterase. *Proc. Natl. Acad. Sci. USA 97:472*.
13. Gardner, C., N. Robas, D. Cawkill, and M. Fidock. 2000. Cloning and characterization of the human and mouse PDE7B, a novel cAMP-specific cyclic nucleotide phosphodiesterase. *Biochem. Biophys. Res. Comm. 272:86*.
14. Glavas, N. A., C. Ostenson, J. B. Schaefer, V. Vasta, and J. A. Beavo. 2001. T cell activation up-regulates cyclic nucleotide phosphodiesterases 8A1 and 7A3. *Proc. Natl. Acad. Sci. USA 98:6319*.
15. Han, P., X. Zhu, and T. Michaeli. 1997. Alternative splicing of the high affinity cAMP-specific phosphodiesterase (PDE7A) mRNA in human skeletal muscle and heart. *J. Biol. Chem. 272:16152*.
16. Li, L., C. Yee, and J. A. Beavo. 1999. CD3- and CD28-dependent induction PDE7 required for T cell activation. *Science 283:848*.
17. Giembycz, M. A., C. J. Corrigan, J. Seybold, R. Newton, and P. J. Barnes. 1996. Identification of cyclic AMP phosphodiesterases 3, 4 and 7 in human $CD4^+$ and $CD8^+$ T-lymphocytes: role in regulating proliferation and the biosynthesis of interleukin-2. *Br. J. Pharmacol. 118:1945*.
18. Ichimura, M., and H. Kase. 1993. A new cyclic nucleotide phosphodiesterase isozyme expressed in the T-lymphocyte cell lines. *Biochem. Biophys. Res. Comm. 193:985*.
19. Zambrowlcz, B. P., G. A. Friedrich, E. C. Buxton, S. L. Lilleberg, C. Person, and A. T. Sands. 1998. Disruption and sequence identification of 2, 000 genes in mouse embryonic stem cells. *Nature 392:608*.
20. Christensen, S. B., A. Guider, C. J. Forster, J. G. Gleason, P. E. Bender, J. M. Karpinski, W. E. DeWolf, Jr., M. S. Barnette, D. C. Underwood, D. E. Griswood, et al. 1998. 1, 4-Cyclohexanecarboxylates: potent and selective inhibitors of phosphodiesterase 4 for the treatment of asthma. *J. Med. Chem. 41:821*.
21. Francis, S. H., J. L. Colbran, L. M. McAllister-Lucas, and J. D. Corbin. 1994. Zinc interaction and conserved motif of the cGMP-binding cGMP-specific phosphodiesterase suggest that it is a zinc hydrolase. *J. Biol. Chem. 269:22477*.
22. Xu, R. X., A. M. Hassell, D. Vanderwall, M. H. Lambert, W. D. Holmes, M. A. Luther, W. J. Rocque, M. V. Milburn, Y. Zhao, H. Ke, and R. T. Nolte. 2000. Atomic structure of PDE4: insights into phosphodiesterase mechanism and specificity. *Science 288:1822*.
23. Lenschow, D. J., T. L. Walunas, and J. A. Bluestone. 1996. CD28/B7 system of T cell costimulation. *Annu. Rev. Immunol. 14:233*.
24. Barnette, M. S., S. B. Christensen, D. A. Essayan, M. Grous, U. Prabhakar, J. A. Rush, A. Kagey-Sobotka, and T. J. Torphy. 1998. SB 207499 (Ariflo), a potent and selective second-generation phosphodiesterase 4 inhibitor: in vitro anti-inflammatory actions. *J. Pharmacol. Exp. Ther. 284:420*.
25. Hatzelmann, A., and C. Schudt. 2001. Anti-inflammatory and immunomodulatory potential of the novel PDE4 inhibitor roflumilast in vitro. *J. Pharmacol. Exp. Ther. 297:267*.
26. Kanka, N., and S. Watanabe. 2001. Regulatory roles of adenylate cyclase and cyclic nucleotide phosphodiesterases 1 and 4 in interleukin-13 production by activated human T cells. *Biochem. Pharmacol. 62:495*.
27. Stein, C. A. 2001. The experimental use of antisense oligonucleotides: a guide for the perplexed. *J. Clin. Invest. 108:641*.
28. Manning, C. D., M. Burman, S. B. Christensen, L. B. Cieslinski, D. M. Essayan, M. Grous, T. J. Torphy, and M. S. Barnette. 1999. Suppression of human inflammatory cell function by subtype-selective PDE4 inhibitors correlates with inhibition of PDE4A and PDE4B. *Br. J. Pharmacol. 128:1393*.
29. Essayan, D. M., S.-K. Huang, B. J. Undem, A. Kagey-Sobotka, and L. M. Litchtenstein. 1994. Modulation of antigen- and mitogen-induced proliferative responses of peripheral blood mononuclear cells by non-selective and isozyme selective cyclic nucleotide phosphodiesterase inhibitors. *J. Immunol. 153:3408*.
30. Martinez, A., A. Castro, C. Gil, M. Miralpeix, V. Segarra, T. Domenech, J. Beleta, J. M. Casacuberta, F. Azorin, B. Pina, and P. Puigdomenech. 2000. Benzyl derivatives of 2, 1, 3-benzo- and benzothieno[3, 2-α]thiadiazine 2, 2-dioxides: first phosphodiesterase 7 inhibitors. *J. Med. Chem. 43:683*.
31. Barnes, M. J., N. Cooper, R. J. Davenport, H. J. Dyke, F. P. Galleway, F. C. A. Galvin, L. Gowers, A. F. Haughan, C. Lowe, J. W. G. Meissner, et al. 2001. Synthesis and structure-activity relationships of guanine analogues as phosphodiesterase 7 (PDE7) inhibitors. *Bioorg. Med. Chem. Lett. 2001:1081*.
32. Dodge, K. L., S. Khouangsathiene, M. S. Kapiloff, R. Mouton, E. V. Hill, M. D. Houslay, L. K. Langeberg, and J. D. Scott. 2001. mAKAP assembles a protein kinase A/PDE4 phosphodiesterase cAMP signaling module. *EMBO J. 20:1921*.
33. MacKenzie, S. J., G. S. Baillie, I. McPhee, G. B. Bolger, and M. D. Houslay. 2000. ERK2 mitogen-activated protein kinase binding, phosphorylation, and regulation of the PDE4D cAMP-specific phosphodiesterases. *J. Biol. Chem. 275:16609*.
34. Perry, S. J., G. S. Baillie, T. A. Kohout, I. McPhee, M. M. Magiera, K. L. Ang, W. E. Miller, A. J. McLean, M. Conti, M. D. Houslay, and R. J. Lefkowitz. 2002. Targeting of cyclic AMP degradation to β2-adrenergic receptors by β-arrestins. *Science 298:834*.
35. Suarez, A., L. Mozo, and C. Gutierrez. 2002. Generation of $CD4^+CD45RA^+$ effector T cells by stimulation in the presence of cyclic adenosine 5′-monophosphate-elevating agents. *J. Immunol. 169:1159*.
36. Suresh, R., M. Vig, S. Bhatia, E. P. Goodspeed, B. John, U. Kandpal, S. Srivastava, A. George, R. Sen, V. Bal, et al. 2002. Pentoxifylline functions as an adjuvant in vivo to enhance T cell immune responses by inhibiting activation-induced death. *J. Immunol. 169:4262*.
37. Lee, R., S. Wolda, E. Moon, J. Esselstyn, C. Hertel, and A. Lerner. 2002. PDE7A is expressed in human B-lymphocytes and is up-regulated by elevation of intracellular cAMP. *Cell. Signal. 14:277*.